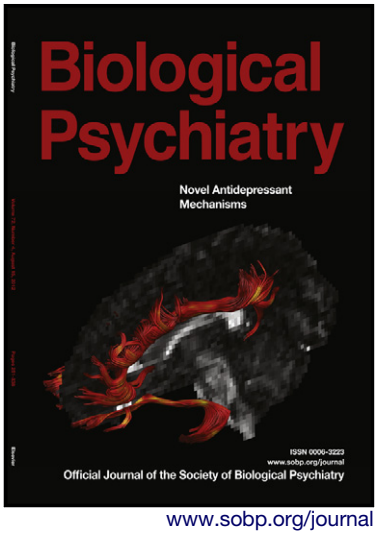

www.sobp.org/journal

Dendritic spine instability in a mouse model of CDKL5 disorder is rescued by IGF-1

Grazia Della Sala, Elena Putignano, Gabriele Chelini, Riccardo Melani, Eleonora Calcagno, Gian Michele Ratto, Elena Amendola, Cornelius T. Gross, Maurizio Giustetto, Tommaso Pizzorusso

PII: S0006-3223(15)00727-1
DOI: http://dx.doi.org/10.1016/j.biopsych.2015.08.028
Reference: BPS12663

To appear in: *Biological Psychiatry*

Cite this article as: Grazia Della Sala, Elena Putignano, Gabriele Chelini, Riccardo Melani, Eleonora Calcagno, Gian Michele Ratto, Elena Amendola, Cornelius T. Gross, Maurizio Giustetto, Tommaso Pizzorusso, Dendritic spine instability in a mouse model of CDKL5 disorder is rescued by IGF-1, *Biological Psychiatry,* http://dx.doi.org/10.1016/j.biopsych.2015.08.028

Dendritic Spine Instability in a Mouse Model of CDKL5 Disorder is rescued by IGF-1

Grazia Della Sala*[1], Elena Putignano*[2], Gabriele Chelini[1], Riccardo Melani[1], Eleonora Calcagno[3], Gian Michele Ratto[4], Elena Amendola[5], Cornelius T. Gross[5], Maurizio Giustetto[£3], Tommaso Pizzorusso[£1,2]

1- Department of Neuroscience, Psychology, Drug Research and Child Health NEUROFARBA University of Florence, Area San Salvi – Pad. 26, 50135 Florence, Italy

2- Institute of Neuroscience, National Research Council (CNR), Via Moruzzi 1, 56124 Pisa, Italy

3 -University of Turin, Department of Neuroscience and National Institute of Neuroscience, Corso M. D'Azeglio 52, 10126 Turin, Italy

4- NEST, Institute of Nanoscience CNR and Scuola Normale Superiore, Pisa, Italy

5- Mouse Biology Unit, European Molecular Biology Laboratory (EMBL), via Ramarini 32, 00015 Monterotondo, Italy

Corresponding author contact information:

Tommaso Pizzorusso, Istituto Neuroscienze CNR, Area Ricerca di Pisa, via Moruzzi, 1 56124 PISA (ITALY). Tel +39-0503153167 Fax +39-0503153220 E-mail: tommaso@in.cnr.it

Running Title: Synaptic impairment in CDKL5 KO mice

*[£] These authors gave equal contribution.

Keywords: Rett syndrome, CDKL5, dendritic spines, imaging, IGF-1, PSD-95

Abstract

Background

CDKL5 (Cyclin-dependent kinase-like 5) is mutated in many severe neurodevelopmental disorders, including atypical Rett syndrome. CDKL5 was shown to interact with synaptic proteins, but an *in vivo* analysis of CDKL5 role in dendritic spine dynamics and synaptic molecular organization is still lacking.

Methods

In vivo 2-photon microscopy of the somatosensory cortex of CDKL5$^{-/y}$ mice was applied to monitor structural dynamics of dendritic spines. Synaptic function and plasticity was measured using electrophysiological recordings of excitatory post-synaptic currents and long-term potentiation (LTP) in brain slices, and assessing the expression of synaptic PSD-95 protein. Finally, we studied the impact of IGF-1 treatment on CDKL5 null mice, to restore the synaptic deficits.

Results

Adult mutant mice showed a significant reduction in spine density and PSD-95-positive synaptic puncta, a reduction of persistent spines and impaired LTP. In juvenile mutants short-term spine elimination but not formation was dramatically increased. Exogenous administration of IGF-1 rescued defective rpS6 phosphorylation, spine density, and PSD-95 expression. Endogenous cortical IGF-1 levels were unaffected by CDKL5 deletion.

Conclusion

These data demonstrate that dendritic spine stabilization is strongly regulated by CDKL5. Moreover, our data suggest that IGF-1 treatment could be a promising candidate for clinical trials in CDKL5 patients.

CDKL5 disorder is a neurodevelopmental pathology with characteristics like intellectual disability, stereotypies, and autism closely related to Rett syndrome (RTT) (1-3), but showing distinctive features such as early onset (first week-5 months of life) epilepsy and severe hypotonia (4). Very little is known about the function of CDKL5 in brain cells. In mice, CDKL5 is expressed at low levels at embryonic stages and its expression is markedly up-regulated during postnatal brain development (5, 6). Expression analysis suggested that CDKL5 can be localized in postsynaptic structures (7) where RNA interference and mutation analysis showed that it can regulate dendritic spine density and morphology and modulate excitatory synaptic function (8). The synaptic localization of CDKL5 seems to be regulated by its direct interaction with the palmitoylated form of postsynaptic density protein 95 (PSD-95) (9, 10), or by the formation of a complex involving PSD-95 and its interacting protein netrin-G1 ligand (NGL-1), a target of CDKL5 kinase activity (8). Recently, CDKL5-loss-of-function murine models that recapitulate some aspects of the human disease have become available (3, 11) making possible to test whether spine and synaptic alterations are present also *in vivo*. Recent studies have shown that adult dendritic spines maintain a significant degree of plasticity undergoing different processes such as formation, elongation, stabilization, and retraction (12,13,14). Thus, to understand the role of CDKL5 in these processes, we analyzed the dynamical changes of dendritic spines in CDKL5$^{-/y}$ mice (11) both during postnatal development and adulthood by means of *in vivo* two photon imaging. Converging evidence showed that CDKL5 absence results in a specific deficit of dendritic spines stabilization that was prominent in juvenile mice and that persisted in the adult. Consistently, the density of dendritic spines was greatly reduced. Spine deficits were accompanied by molecular and functional synaptic alterations consisting in a reduction of synaptic PSD-95, impaired LTP maintenance, and reduced spontaneous EPSC frequency.

No cure is currently available for CDKL5 patients and no treatment has been attempted so far to modulate the phenotype of CDKL5$^{-/y}$ mice. Considering the strong impairment in dendritic spine stability observed in juvenile CDKL5$^{-/y}$ mice, we used this phenotype to evaluate the effects

of a treatment aimed at ameliorating CDKL5$^{-/y}$ mice condition. Insulin-like growth factor 1 (IGF-1) is an activator of the Akt-mTOR pathway (15, 16) a molecular cascade involved in several neurodevelopmental disorders that is hypofunctional in CDKL5$^{-/y}$ mice (11). Moreover, IGF-1 treatment was found to ameliorate spine dynamics and behavioural phenotype in murine models of RTT involving MeCP2 deletion (17, 18) and a clinical trial is ongoing in MeCP2 patients (19). We found that systemic IGF-1 treatment restored spine density, spine elimination rate, and synaptic PSD-95 levels in CDKL5$^{-/y}$ mice, thus candidating IGF-1 as a treatment for CDKL5 disorder.

Materials and Methods

Mice were handled according to protocols approved by the Italian Ministry of Health. All mice were kept in a normal 12 h light/dark cycle in a temperature–controlled room (20°C) and had access to food and water *ad libitum*. The CDKL5 null line of mice (11) was crossed with Thy-1 GFP transgenic mice (line M) (20) to produce the experimental animals: homozygous mutant (CDKL5$^{-/y}$) males and their CDKL5$^{+/y}$ littermates.

Surgery: In order to acquire images of the dendritic spines of the somatosensory cortex, mice underwent surgery to grant optical access to the living cortex (21). Mice were anaesthetized with an intraperitoneal injection (1 ml per 0.05 kg body weight) of avertin. Mice were treated with carprofen (Rimadyl, Pfizer, daily i.p. injections of 0.3 ml from a 0.50 mg ml^{-1} stock), starting immediately before the cranial window implantation (see supplementary online material).

In vivo two-photon imaging: Imaging sessions were carried out on a 2-photon microscope setup obtained by fitting a 5 W laser (Mira, Coherent) tuned at 890 nm that delivered 20-30 mW at the sample on a Olympus Fluoview confocal microscope. A CCD (charge-coupled device) camera was used to acquire a high-quality picture of the brain vasculature, which was used as a landmark for future relocation. Two-photon imaging was restricted to the apical dendrites of layer V pyramidal neurons present in cortical layers II/III (50–200 μm below the cortical surface). Images was acquired with a water immersion lens (Olympus 20×, NA 0.95) and digitized at a resolution of 1024x1024 pixels at zoom 10x. The stack step size was 0.475 μm (22).

IGF-1 treatment: Subcutaneous injections of 2-4 microliters of a solution of full-length IGF-1 (IU100; 1.8 µg/g body weight; Biovision) solved in saline were delivered to in CDKL5$^{+/y}$ and CDKL5$^{-/y}$ mice (17, 22). To study IGF-1 effect in young mice we performed a single injection daily for 4 days from P24 to P27 and the imaging was performed at P27 and P28. For the adult study we injected IGF-1 daily between the first two imaging sessions (P120-P124*)*. Subcutaneous injections were performed using a catheter with a 20 gauge needle connected to a Hamilton syringe.

Results

Decreased density of dendritic spines in pyramidal neurons of CDKL5$^{-/y}$ mice.

We implanted P30 GFP positive CDKL5$^{-/y}$ and CDKL5$^{+/y}$ mice with a cranial window overlying the somatosensory cortex. The apical dendritic tufts of layer V pyramidal cells were repeatedly acquired between P50 and P80 during five imaging sessions (Figure 1A).

At all ages, CDKL5$^{-/y}$ mice (n=8, 492 spines) had a significantly lower dendritic spine density than CDKL5$^{+/y}$ (n=7, 789 spines) (figure 1B-C; two-way ANOVA factor genotype: $F(1,57)=77.55$, $p<0.001$, 28 dendrites for CDKL5$^{+/y}$, 31 for CDKL5$^{-/y}$, post hoc Bonferroni t-test, $p<0.001$). Intriguingly, the factor age seemed to have a significantly different effect within each genotype (two-way ANOVA interaction age × genotype: $F(4,227)=8.077$, $p<0.001$). Indeed, linear fits of the spine density as a function of age for individual dendrites revealed that in CDKL5$^{+/y}$ mice spine density was virtually constant during the period of observation (slope: 0.0017± 0.0014 spines/µm/day; one sample t-test $t(27)=1.2$, $p=0.24$), whilst spine density of mutant mice showed a significant decrease with time (slope: -0.0052± 0.0009 spines/µm/day; one sample t test $t(30) = -5.56$, $p<0.001$). These data suggest that adult CDKL5$^{-/y}$ mutants show a relatively small but significant reduction in spine density during the 30 days period of observation.

To understand whether synaptic contacts are also affected in CDKL5$^{-/y}$ mice, we performed immunofluorescence experiments analyzing the localization of PSD-95, a postsynaptic marker of excitatory synapses (Figure S1). The data showed that CDKL5$^{-/y}$ mice displayed a strong reduction of PSD-95-positive synaptic puncta (n=6 each group, layer II-III $t(10)=2.46$ t-test $p=0.008$, layer V $t(10)=2.44$ t-test $p=0.011$) both in layer II-III and V of the somatosensory cortex (Figure 1 D-E) indicating that CDKL5 deletion causes a robust loss of excitatory synaptic contacts.

Impairment of long-term spine survival in CDKL5$^{-/y}$ mice

To dissect out the role of CDKL5 in spine formation and elimination (23), we measured the fraction of spines undergoing formation and elimination over 4 days by comparing dendrites at P50 with those at P54. Figure S2 shows that there is no effect of genotype neither on spine gain (t-test p=0.21; t(57)=1.27), nor on spine loss (t-test p=0.88, t(57)=0.14) indicating that CDKL5 effect on spine stability in adult mice cannot be detected with this short time interval.

Next, we analyzed if CDKL5 can be implicated in long-term maintenance of persistent dendritic spines. To this aim, we tracked the fate of individual spines observed in the first imaging session (P50) and calculated the fraction of spines surviving (survival fraction) at the subsequent imaging sessions until P80 (Figure 2A). At the end of the examination period (P80), only 64% of the spines that were observed at P50 had survived in the CDKL5$^{-/y}$ mice, whereas the control littermates displayed a survival rate of 75%. We fitted the data with an exponential function with the parameter S corresponding to the asymptotic survival fraction, and the parameter τ corresponding to the time constant necessary to lose 37% of the spines bound to disappear (21) (Figure 2B). Figure 2C shows that CDKL5$^{-/y}$ group had a significantly lower S parameter (t-test, t(50)=2.9 p=0.005) and longer τ (t-test, t(50)=-2.82 p=0.006) than CDKL5$^{+/y}$ suggesting that dendritic spines require more days to become stable in CDKL5$^{-/y}$ mice. The lack of stability of CDKL5$^{-/y}$ spines is also apparent by comparing spine survival at the two final imaging sessions. Whereas surviving spines reached a plateau and did not change significantly in CDKL5$^{+/y}$ mice (t-test, t(54)= 0.85 p=0.39), surviving spines continued to decrease in CDKL5$^{-/y}$ mice (t-test, t(60)=2.32 p=0.02). To further investigate this point, we measured the fraction of spines gained during the imaging sessions and persisting for at least 8 days (new persistent, NP). We found that NP spines were present at significantly lower level in CDKL5$^{-/y}$ mice than controls (Figure 2D) (X^2(1)= 6.76; p=0.009*)*. In agreement with a reduced long-term spine stability in CDKL5$^{-/y}$ mice, morphological analysis of dendritic spines revealed the presence of characteristics of immature spines (12) in CDKL5$^{-/y}$ mice. Indeed, spine neck was significantly longer and spine head

significantly smaller in CDKL5$^{-/y}$ than in controls mice (Figure 2E-F) (length t-test t(177)=-1.95 p=0.05; head width t-test t(177)=2.92 p=0.003). Thus, long-term survival of dendritic spines is impaired in adult CDKL5$^{-/y}$ mice.

Impaired synaptic transmission and plasticity in CDKL5$^{-/y}$ mice

We investigated synaptic plasticity in GFP-positive adult CDKL5$^{-/y}$ mice. Acute somatosensory cortex slices of P80 mutant and wild-type mice were used to study LTP of field potentials evoked by stimulating the horizontal connections in layer II-III. After I/O curve assessment, stimulation intensity was chosen to evoke half-maximal response. Neither the I/O curve (fig. S3) nor stimulation intensity (CDKL5$^{+/y}$ 158±29 µA; CDKL5$^{-/y}$ 149±19 µA, t-test t(10)=0.27 p=0.79) were different between CDKL5$^{+/y}$ and CDKL5$^{-/y}$ mice. In CDKL5$^{+/y}$ mice, theta burst stimulation resulted in a robust LTP induction whereas CDKL5$^{-/y}$ mice showed a dramatic impairment of LTP expression (Figure 3, 8 slices from 8 CDKL5$^{+/y}$ mice, 4 slices from 4 CDKL5$^{-/y}$ mice; two-way ANOVA time × genotype p<0.001 F(1,10)=25.0 post-hoc Holm-Sidak comparison p<0.001 t(10)=7.07).

We then studied excitatory synaptic transmission by recording spontaneous mini-EPSCs (mEPSCs). mEPSCs were recorded by whole-cell recordings targeted to GFP-labelled layer V pyramidal cells of somatosensory cortex slices of CDKL5$^{-/y}$ and CDKL5$^{+/y}$ mice. No difference was present in resting potential and input resistance (Table 1). mEPSCs from CDKL5$^{+/y}$ neurons had an average mEPSC frequency that was significantly higher than CDKL5$^{-/y}$ mice (Figure 4B-C) with shorter inter-event intervals (Figure 4E, Kolmogorov-Smirnov test, D=0.454, p<0.001). mEPSC median amplitude was similar between CDKL5$^{-/y}$ and CDKL5$^{+/y}$ mice (amplitude t-test t(21)=-0.141 p=0.45; frequency t(21)=2.22 p=0.039; 12 slices from 4 CDKL5$^{+/y}$ mice; 11 slices from 5 CDKL5$^{-/y}$ mice) (Figure 4A); however, the cumulative distribution of mEPSCs amplitudes for CDKL5$^{+/y}$ mice is significantly shifted towards larger values respect to CDKL5$^{-/y}$ mice (Kolmogorov-Smirnov test, D=0.406, p<0.001, Figure 4D).

Dendritic spine density is already affected in developing CDKL5$^{-/y}$

We studied whether dendritic spine density and dynamics in mutant mice during development (P27-P28). Since at this age it is not possible to provide an interval of 20 days between cranial window implantation and imaging, we imaged dendritic spines using the thinned skull approach (24).

As shown in figure 5A-B, at P27 CDKL5$^{-/y}$ mice displayed significantly less spine density than CDKL5$^{+/y}$ littermates (t-test t(115)=4.03; p<0.0001; n=62 dendrites from 20 CDKL5$^{+/y}$ mice; 55 dendrites from 23 CDKL5$^{-/y}$ mice). By contrast, the density of filopodia was similar between the two genotypes (t-test t(115)=-0.24; p=0.81), suggesting that CDKL5 is not involved in the production of new spines but, rather in the stabilization of spines with mature morphology. Indeed, spines of mushroom-like morphology, that are considered to be mature spines, were significantly increased in CDKL5$^{+/y}$ with respect to CDKL5$^{-/y}$ (t-test, t(29)=2.78 p=0.009). To assess whether the decrease in spine number was reflected by a reduction in excitatory synaptic contacts, we performed immunofluorescence experiments for the excitatory synaptic marker PSD-95. The data showed (Figure 5 C-D) that CDKL5$^{-/y}$ mice displayed a reduction of PSD-95-positive puncta both in layer II-III and V of somatosensory cortex already at P28 (n=6 for each group, layer II-III t-test p=0.002 t(10)=2.96, layer V t-test p=0.006 t(10)=1.89).

Enhanced short-term loss of dendritic spines in developing CDKL5$^{-/y}$ mice

To investigate spine dynamics in developing CDKL5$^{-/y}$ mice we calculated dendritic spine gain and loss between two imaging sessions separated by one day beginning at P27 (Figure 6 A-C). We found that the fraction of spines gained in 24 hours is similar between the two genotypes (t-test t(43)=0.15 p=0.87). Conversely, the fraction of lost spines was greatly increased in the mutant mice respect to wt littermates (t-test t(43)=-2.95 p=0.005; n=21 dendrites, from 11 CDKL5$^{+/y}$ mice, 570

spines; 24 dendrites from 14 CDKL5$^{-/y}$ mice, 487 spines). Thus, CDKL5 plays a crucial role in limiting short term pruning of dendritic spines during development.

IGF-1 administration rescues defective PSD-95 expression and S6 phosphorylation in CDKL5$^{-/y}$ mice

IGF-1 is an activator of Akt/mTOR/S6 pathway (16) that was found to have beneficial effects in murine models of RTT involving MeCP2 deletion (17, 18). Therefore, we investigated the effects of IGF-1 on S6 phosphorylation (11) in the somatosensory cortex. We followed a protocol of IGF-1 administration with daily doses of 1.8 µg/g body weight from P24 to P27 that we previously showed to be able to improve spine motility in MeCP2 mutants (22). Phosphorylation of Ser240-244 residues of S6 ribosomal protein (n=8-9 animals for group) is specifically induced by the action of the mTOR/PI3K pathway (25). S6 Ser240-244 phosphorylation was reduced in CDKL5$^{-/y}$ mice treated with vehicle with respect to CDKL5$^{+/y}$, however IGF-1 treatment rescued S6 phosphorylation to normal levels. (Figure 7A-B, two-way ANOVA; factor genotype $F(1,30)=4,41$ $p=0.044$; treatment $F(1,30)=19,1$ $p<0,001$; interaction treatment × genotype $F(1,33)=0,013$ $p=0.9$; post-hoc Holm-Sidak comparisons: genotype within vehicle $t=2.15$ $p=0.039$, genotype within IGF-1 $t=1.15$ $p=0.25$, treatment within CDKL5$^{-/y}$ $t=3.25$ $p=0.003$, treatment within CDKL5$^{+/y}$ $t=2.93$ $p=0.006$).

Previous work showed that IGF-1 can rescue deficits in PSD-95 synaptic expression in models of RTT carrying deletion of MeCP2 (18). Thus, we studied whether IGF-1 could improve the PSD-95 deficit observed in CDKL5$^{-/y}$ mice. We extracted the PSD fraction from synaptosomes and we assessed PSD-95 by western blot (n=9 animals for group). Vehicle treated CDKL5$^{-/y}$ had less PSD-95 than CDKL5$^{+/y}$, however IGF-1 rescued PSD-95 reduction (Figure 7C-D, two-way ANOVA; factor genotype $F(1,28)=7,99$ $p=0.009$; treatment $F(1,28)=8,64$ $p=0.007$, interaction treatment × genotype $F(1,31)=0,029$ $p=0.85$, post-hoc comparison genotype within vehicle $t=2.06$

p=0.049, genotype within IGF-1 t=2.05 p=0.049, treatment within CDKL5$^{-/y}$ t=2.07 p=0.048, treatment within CDKL5$^{+/y}$ t=2.19 p=0.037).

Finally, we analyzed cortical levels of IGF-1 in both P27 and P90 CDKL5$^{-/y}$ mice. No difference of IGF-1 expression was observed between CDKL5$^{+/y}$ and CDKL5$^{-/y}$ (Figure 7E,F), suggesting that IGF-1 effects in CDKL5$^{-/y}$ mice are not due to a restoration of altered cortical IGF-1 levels.

IGF-1 administration rescues spine density and turnover in developing and adult CDKL5$^{-/y}$ mice

We then asked whether IGF-1 delivery could rescue the dendritic spine deficits of CDKL5$^{-/y}$ mice. To assess the effects of IGF-1 in juvenile mice spine imaging was performed at P27 and P28 (Figure 8A, experimental time line) in four experimental groups: CDKL5$^{+/y}$ and CDKL5$^{-/y}$, injected with vehicle or IGF-1 (CDKL5$^{+/y}$ vehicle, 27 dendrites from 6 mice, 968 spines; CDKL5$^{-/y}$ vehicle, 25 dendrites from 8 mice, 668 spines; CDKL5$^{+/y}$ IGF-1, 20 dendrites from 7 mice, 695 spines; CDKL5$^{-/y}$ IGF-1, 40 dendrites from 12 mice, 1191 spines). The analysis of spine density revealed a significant effect of genotype and a significant interaction treatment × genotype (Figure 8B, two-way ANOVA, factor genotype F(1,104)=13.71 p<0.001; interaction treatment x genotype F(1,107)=5.06 p=0.02). No main effect of treatment was present (factor treatment F(1,104)= 2.63 p=0.10). As expected from our previous results, post-hoc comparisons revealed that CDKL5$^{-/y}$ mice treated with vehicle showed reduced spine density with respect to CDKL5$^{+/y}$ vehicle treated mice (Holm-Sidak test p<0.001, t(47)= 4.14). Intriguingly, IGF-1 significantly enhanced spine density of CDKL5$^{-/y}$ mice with respect to vehicle treated CDKL5$^{-/y}$ mice (Holm-Sidak p=0.004 t(59)= 2.91). Spine turnover analysis (CDKL5$^{+/y}$ vehicle 13 dendrites from 6 mice; CDKL5$^{-/y}$ vehicle 19 dendrites from 7 mice; CDKL5$^{+/y}$ IGF-1 10 dendrites from 5 mice; CDKL5$^{-/y}$ IGF-1 21 dendrites from 7 mice) revealed that spine loss was significantly affected by the genotype with an interaction

genotype x treatment (two-way ANOVA; factor genotype $F(1,55)=3.93$ $p=0.05$; interaction treatment × genotype $F(1,58)= 4.21$ $p=0.04$). Post-hoc comparisons showed that, as in untreated mice, CDKL5$^{-/y}$ mice treated with vehicle had an abnormally high rate of spine loss as compared with vehicle treated CDKL5$^{+/y}$ (Figure 8 C-D, Holm-Sidak test $p=0.004$ $t(28)=3.04$). By contrast, spine loss was fully rescued in the CDKL5$^{-/y}$ mice treated with IGF-1 (Holm-Sidak test $p=0.002$ $t(37)=3.30$). No effect of genotype or treatment was present on spine gain (two-way ANOVA; factor treatment $F(1,55)=0.46$ $p=0.49$; factor genotype $F(1,55)=0.88$ $p=0.35$; interaction treatment × genotype $F(1,58)=2.48$ $p=0.12$). Thus, the spine deficit phenotype of juvenile CDKL5$^{-/y}$ can be counteracted by IGF-1.

We next asked if the beneficial effect of IGF-1 can occur also in adult CDKL5$^{-/y}$ mice. After cranial window implantation at P30, dendritic spines of CDKL5$^{-/y}$ mice were imaged at P120 (Figure 9A). Mice were then randomly assigned to the IGF-1 or the vehicle group (n=5 mice per group). Immediately at the end of the treatment (P124) spine density showed a significant increase in the IGF-1 group (Figure 9B). By contrast, vehicle treated CDKL5$^{-/y}$ mice showed the reduction in dendritic spine density observed also in untreated CDKL5$^{-/y}$ mice. Spine turnover analysis (Figure 9C) revealed that spine increase was due to reduced spine loss ($t(77)=2.82$ $p=0.005$) and also to an increase in spine gain ($t(77)=3.21$ $p=0.001$). These data show that IGF-1 is effective on spine density also in adult CDKL5$^{-/y}$ mice.

To assess whether the spine density increase induced by IGF-1 could persist after the end of the treatment we imaged again the same dendrites 16 and 20 days after the end of the treatment (P140 and P144). IGF-1 treated mice maintained significantly more spines than vehicle treated mice at these time points (Figure 9B; two way ANOVA effect of time $F(2,175)=5.06$ $p=0.007$; effect of treatment $F(2,175)=30.99$ $p<0.001$; post hoc comparisons: IGF-1 was significantly different from vehicle at P124 $t=4.63$ $p<0.001$, P140 $t=2.24$ $p=0.003$, and P144 $t=3.18$ $p=0.002$).

Discussion

Our study shows that CDKL5, a protein that when mutated causes atypical RTT, plays a crucial role in the organization and maintenance of synaptic structure *in vivo*. By performing repeated *in vivo* two-photon imaging in CDKL5$^{-/y}$ mice (11), we pinpointed the cellular process affected by CDKL5 absence. Indeed, new spines were normally generated but failed to stabilize and were eliminated at abnormally high rate in the absence of CDKL5. This deficit resulted in a strong decrease in spine density of pyramidal cells, nearly half as much, that was accompanied by a decrease of PSD-95-positive puncta together with a reduction of PSD-95 expression in the PSD enriched fraction of synaptosomes. Morphological and molecular alterations of synapses were reflected by functional impairments consisting in a reduction in the frequency of miniature EPSCs, possibly due to decreased synapse number, and defective LTP.

Previous studies performed in neuronal cultures converged in identifying mechanisms of synaptic stabilization involving PSD-95 as a target of CDKL5 action. It was found that CDKL5 is present at excitatory synapses where it is necessary to phosphorylate the cell adhesion molecule NGL-1 (8). In turn, NGL-1 phosphorylation would be necessary to produce a stable association between NGL-1 and PSD-95 promoting synaptic stabilization and formation of mature dendritic spines. Indeed, the authors found a decrease of mature dendritic spine density in response to CDKL5 knockdown in neuronal cultures and in the P11 cortex *in vivo*. The presence of spine alterations during early development suggests that the impairment of dendritic spine maturation represents a primary phenotype induced by CDKL5 mutation. Intriguingly, the authors also observed that overall dendritic protrusion density was increased, suggesting that at early developmental stages CDKL5 could also play a role in limiting filopodia outgrowth or that the excess protrusions present after CDKL5 knockdown represent atrophic spines unable to complete the maturation process leading to a stable spine. Importantly, an alteration in dendritic spine formation was also observed in neurons derived from induced pluripotent stem cells reprogrammed from patient fibroblasts suggesting that spine and synaptic abnormalities are likely present also in

patients (8). Zhu and colleagues proposed that CDKL5 directly interacts with PSD-95 in a PSD-95 palmitoylation-dependent way and that this interaction targets CDKL5 to excitatory synapses (10). Pathogenic mutations of CDKL5, by interfering with this mechanism, resulted in impaired spine maturation and reduced spine density in cultured neurons (10). Our *in vivo* data showing decreased synaptic PSD-95 clusters could be explained by these molecular models of CDKL5 action at postsynaptic sites. Moreover, *in vivo* data showed that newly formed spines that failed to acquire well clustered PSD-95 rarely survived for more than one day (26). Thus, impaired PSD-95 stabilization in our CDKL5 mutant mice could also promote the excessive spine elimination that we observe in juvenile mice. CDKL5 is clearly important for spine stability also in adult animals as persistent spines were significantly reduced in CDKL5 mutants. Even in mature spines a smaller PSD-95 positive PSD was observed well before the actual pruning event in those spines that were doomed to disappear (26), raising the possibility that this mechanism could explain the long-term instability that we observed in adult CDKL5 mutants. Taken together these observations suggest that, like MeCP2 (27, 28), CDKL5 could have a lifelong role on neuronal function.

The dependence of CDKL5 binding of PSD-95 upon PSD-95 palmitoylation suggests the possibility that CDKL5 dynamically interacts with PSD-95 in an activity-dependent way (9). It has been previously shown that palmitate cycling on PSD-95 is regulated by electrical activity and can control synaptic strength and activity-dependent plasticity (29). Our experiments showing a dramatic LTP impairment in CDKL5$^{-/y}$ mice cortex are in line with this hypothesis. Overall our results add to those of the literature reinforcing the idea that CDKL5 disease is caused from a deficit of impaired synaptic organization and plasticity, similarly to what happens in classical RTT caused by mutations of MeCP2 gene (30).

It has to be underscored that other molecular alterations can be induced by CDKL5 mutations (7). For instance, the analysis of the genetic models of CDKL5 deletion reported deficits in the activation of several kinases (3, 11). In particular, phosphorylation of Ser240-244 of S6, a specific target of the AKT-mTOR pathway, is downregulated in CDKL5 mutants, a feature also

shared by RTT models carrying MeCP2 deletion (3, 11, 31). IGF-1 is a potential activator of this pathway (18, 32, 33) and treatment with IGF-1 improves organism function, specific behaviors, cellular pathway activation, and synaptic plasticity in mice model of RTT syndrome (19, 34) and Phelan-McDermid syndrome, a syndrome caused by mutations of PSD-95 binding protein Shank-3 (35). In particular, MeCP2 mutant mice were found to have an impaired spine motility and formation (22, 36). Also in this case, IGF-1 was able to rescue the spine impairment present in MeCP2 null mice (22). Our experiments show that IGF-1 is able to rescue S6 phosphorylation, spine deficits and PSD-95 decrease also in CDKL5$^{-/y}$ mice. Synaptic PSD-95 expression was increased by IGF-1 also in CDKL5$^{+/y}$ mice whereas spine density was not affected, suggesting that each synapse could have more PSD-95 or more PSD-95 puncta are present on the same spine or along dendritic shafts. These molecular alterations of CDKL5$^{-/y}$ mice do not seem to be due to lower-than-normal levels of endogenous IGF-1 because we found normal cortical IGF-1 levels in CDKL5$^{-/y}$ mice. Thus, the effects of exogenous IGF-1 could be brought about by a potentiation of defective signalling pathways, such as those converging on S6 phosphorylation.

Importantly, IGF-1 improved spine density also in adult CDKL5$^{-/y}$ mice when the synaptic deficit is established. Moreover, repeated imaging of the same dendrites before and after the IGF-1 treatment showed that the increased spine density induced by IGF-1 was still present 20 days after the end of the IGF-1 treatment suggesting that the spines induced by IGF-1 are long-lasting.

The results of a phase 1 study on the use of IGF-1 in patients affected by classical RTT caused by MeCP2 mutations has been recently published (19). Our results prompt a thorough investigation of the IGF-1 effects in CDKL5 disease preclinical models and possibly to establish a firm background for a clinical use of IGF-1 also in girls carrying CDKL5 mutations.

Acknowledgments:

This work was supported by the EU 7th Framework Programme [FP2007-2013] under grant agreements no 223326 and 223524, the MIUR-CNR flagship project EPIGEN, Associazione Italiana Sindrome di Rett, Telethon project GGP1114, VALCOMP Regione Toscana project POR CRO FSE 2007-2013 Asse IV - Capitale Umano, Associazione Albero di Greta, ONLUS, Fondazione San Paolo.

Financial Disclosures

All authors report no biomedical financial interests or potential conflicts of interest.

References

1. Bertani I, Rusconi L, Bolognese F, Forlani G, Conca B, De Monte L, et al. (2006): Functional consequences of mutations in CDKL5, an X-linked gene involved in infantile spasms and mental retardation. *J Biol Chem*. 281:32048-32056.

2. Mari F, Azimonti S, Bertani I, Bolognese F, Colombo E, Caselli R, et al. (2005): CDKL5 belongs to the same molecular pathway of MeCP2 and it is responsible for the early-onset seizure variant of Rett syndrome. *Hum Mol Genet*. 14:1935-1946.

3. Wang IT, Allen M, Goffin D, Zhu X, Fairless AH, Brodkin ES, et al. (2012): Loss of CDKL5 disrupts kinome profile and event-related potentials leading to autistic-like phenotypes in mice. *Proc Natl Acad Sci U S A*. 109:21516-21521.

4. Bahi-Buisson N, Nectoux J, Rosas-Vargas H, Milh M, Boddaert N, Girard B, et al. (2008): Key clinical features to identify girls with CDKL5 mutations. *Brain*. 131:2647-2661.

5. Rusconi L, Salvatoni L, Giudici L, Bertani I, Kilstrup-Nielsen C, Broccoli V, et al. (2008): CDKL5 expression is modulated during neuronal development and its subcellular distribution is tightly regulated by the C-terminal tail. *J Biol Chem*. 283:30101-30111.

6. Chen Q, Zhu YC, Yu J, Miao S, Zheng J, Xu L, et al. (2010): CDKL5, a protein associated with rett syndrome, regulates neuronal morphogenesis via Rac1 signaling. *J Neurosci*. 30:12777-12786.

7. Ricciardi S, Kilstrup-Nielsen C, Bienvenu T, Jacquette A, Landsberger N, Broccoli V (2009): CDKL5 influences RNA splicing activity by its association to the nuclear speckle molecular machinery. *Hum Mol Genet*. 18:4590-4602.

8. Ricciardi S, Ungaro F, Hambrock M, Rademacher N, Stefanelli G, Brambilla D, et al. (2012): CDKL5 ensures excitatory synapse stability by reinforcing NGL-1-PSD95 interaction in the

postsynaptic compartment and is impaired in patient iPSC-derived neurons. *Nat Cell Biol*. 14:911-923.

9. Zhang Y, Matt L, Patriarchi T, Malik ZA, Chowdhury D, Park DK, et al. (2014): Capping of the N-terminus of PSD-95 by calmodulin triggers its postsynaptic release. *EMBO J*. 33:1341-1353.

10. Zhu YC, Li D, Wang L, Lu B, Zheng J, Zhao SL, et al. (2013): Palmitoylation-dependent CDKL5-PSD-95 interaction regulates synaptic targeting of CDKL5 and dendritic spine development. *Proc Natl Acad Sci U S A*. 110:9118-9123.

11. Amendola E, Zhan Y, Mattucci C, Castroflorio E, Calcagno E, Fuchs C, et al. (2014): Mapping pathological phenotypes in a mouse model of CDKL5 disorder. *PLoS One*. 9:e91613.

12. Holtmaat AJ, Trachtenberg JT, Wilbrecht L, Shepherd GM, Zhang X, Knott GW, et al. (2005): Transient and persistent dendritic spines in the neocortex in vivo. *Neuron*. 45:279-291.

13. Holtmaat A, De Paola V, Wilbrecht L, Knott GW (2008): Imaging of experience-dependent structural plasticity in the mouse neocortex in vivo. *Behav Brain Res*. 192:20-25.

14. Holtmaat A, de Paola V, Wilbrecht L, Trachtenberg JT, Svoboda K, Portera-Cailliau C (2012): Imaging neocortical neurons through a chronic cranial window. *Cold Spring Harb Protoc*. 2012:694-701.

15. Laviola L, Natalicchio A, Giorgino F (2007): The IGF-I signaling pathway. *Curr Pharm Des*. 13:663-669.

16. Chen J, Alberts I, Li X (2014): Dysregulation of the IGF-I/PI3K/AKT/mTOR signaling pathway in autism spectrum disorders. *Int J Dev Neurosci*. 35:35-41.

17. Tropea D, Giacometti E, Wilson NR, Beard C, McCurry C, Fu DD, et al. (2009): Partial reversal of Rett Syndrome-like symptoms in MeCP2 mutant mice. *Proc Natl Acad Sci U S A*. 106:2029-2034.

18. Castro J, Garcia RI, Kwok S, Banerjee A, Petravicz J, Woodson J, et al. (2014): Functional recovery with recombinant human IGF1 treatment in a mouse model of Rett Syndrome. *Proc Natl Acad Sci U S A*. 111:9941-9946.

19. Khwaja OS, Ho E, Barnes KV, O'Leary HM, Pereira LM, Finkelstein Y, et al. (2014): Safety, pharmacokinetics, and preliminary assessment of efficacy of mecasermin (recombinant human IGF-1) for the treatment of Rett syndrome. *Proc Natl Acad Sci U S A*. 111:4596-4601.

20. Feng G, Mellor RH, Bernstein M, Keller-Peck C, Nguyen QT, Wallace M, et al. (2000): Imaging neuronal subsets in transgenic mice expressing multiple spectral variants of GFP. *Neuron*. 28:41-51.

21. Holtmaat A, Bonhoeffer T, Chow DK, Chuckowree J, De Paola V, Hofer SB, et al. (2009): Long-term, high-resolution imaging in the mouse neocortex through a chronic cranial window. *Nat Protoc*. 4:1128-1144.

22. Landi S, Putignano E, Boggio EM, Giustetto M, Pizzorusso T, Ratto GM (2011): The short-time structural plasticity of dendritic spines is altered in a model of Rett syndrome. *Sci Rep*. 1:45.

23. Holtmaat A, Wilbrecht L, Knott GW, Welker E, Svoboda K (2006): Experience-dependent and cell-type-specific spine growth in the neocortex. *Nature*. 441:979-983.

24. Yang G, Pan F, Parkhurst CN, Grutzendler J, Gan WB (2010): Thinned-skull cranial window technique for long-term imaging of the cortex in live mice. *Nat Protoc*. 5:201-208.

25. Ruvinsky I, Meyuhas O (2006): Ribosomal protein S6 phosphorylation: from protein synthesis to cell size. *Trends Biochem Sci*. 31:342-348.

26. Cane M, Maco B, Knott G, Holtmaat A (2014): The relationship between PSD-95 clustering and spine stability in vivo. *J Neurosci*. 34:2075-2086.

27. McGraw CM, Samaco RC, Zoghbi HY (2011): Adult neural function requires MeCP2. *Science*. 333:186.

28. Guy J, Gan J, Selfridge J, Cobb S, Bird A (2007): Reversal of neurological defects in a mouse model of Rett syndrome. *Science*. 315:1143-1147.

29. El-Husseini D, Schnell E, Dakoji S, Sweeney N, Zhou Q, Prange O, et al. (2002): Synaptic strength regulated by palmitate cycling on PSD-95. *Cell*. 108:849-863.

30. Della Sala G, Pizzorusso T (2014): Synaptic plasticity and signaling in rett syndrome. *Dev Neurobiol*. 74:178-196.

31. Ricciardi S, Boggio EM, Grosso S, Lonetti G, Forlani G, Stefanelli G, et al. (2011): Reduced AKT/mTOR signaling and protein synthesis dysregulation in a Rett syndrome animal model. *Hum Mol Genet*. 20:1182-1196.

32. Nishijima T, Piriz J, Duflot S, Fernandez AM, Gaitan G, Gomez-Pinedo U, et al. (2010): Neuronal activity drives localized blood-brain-barrier transport of serum insulin-like growth factor-I into the CNS. *Neuron*. 67:834-846.

33. Vandomme J, Touil Y, Ostyn P, Olejnik C, Flamenco P, El Machhour R, et al. (2014): Insulin-like growth factor 1 receptor and p38 mitogen-activated protein kinase signals inversely regulate signal transducer and activator of transcription 3 activity to control human dental pulp stem cell quiescence, propagation, and differentiation. *Stem Cells Dev*. 23:839-851.

34. Mellios N, Woodson J, Garcia RI, Crawford B, Sharma J, Sheridan SD, et al. (2014): beta2-Adrenergic receptor agonist ameliorates phenotypes and corrects microRNA-mediated IGF1 deficits in a mouse model of Rett syndrome. *Proc Natl Acad Sci U S A*. 111:9947-9952.

35. Shcheglovitov A, Shcheglovitova O, Yazawa M, Portmann T, Shu R, Sebastiano V, et al. (2013): SHANK3 and IGF1 restore synaptic deficits in neurons from 22q13 deletion syndrome patients. *Nature*. 503:267-271.

36. Jiang M, Ash RT, Baker SA, Suter B, Ferguson A, Park J, et al. (2013): Dendritic arborization and spine dynamics are abnormal in the mouse model of MECP2 duplication syndrome. *J Neurosci*. 33:19518-19533.

Figure Captions

Figure 1. *Synaptic alterations in adult CDKL5$^{-/y}$ mice.* ***A****, Experimental time line for in vivo imaging.* ***B****, Image of a dendritic branch from a CDKL5$^{+/y}$ and CDKL5$^{-/y}$ mice at P50, showing decrease spine density.* ***C****, Mean spine density from P50 until P80 in CDKL5$^{+/y}$ and CDKL5$^{-/y}$ mice. CDKL5$^{-/y}$ mice always displayed lower spine densities compared with CDKL5$^{+/y}$ littermates.* ***D****, Confocal images of PSD-95 puncta detected by immunohistochemistry in CDKL5$^{+/y}$ and CDKL5$^{-/y}$ mice.* ***E****, Quantification of PSD-95 puncta (number of PSD-95 puncta/micron^2) in the layer II-III and V of somatosensory cortex of CDKL5$^{+/y}$ and CDKL5$^{-/y}$ mice.*

Figure 2. *Spine stabilization is affected in adult CDKL5$^{-/y}$ mice.* ***A,*** *Images of a dendritic branch from a CDKL5$^{+/y}$ and CDKL5$^{-/y}$ mice at the beginning (P50) and at the end of the imaging period (P80). Yellow arrows indicate that spines that survived through this period. Red arrows indicate spines that are lost over time (scale bar 2 μm).* ***B,*** *Survival fraction of spines present at P50 and then monitored at P54, P58, P65 and P80 both in CDKL5$^{+/y}$ (black) and CDKL5$^{-/y}$ mice (grey). Continuous lines are exponential fits of the data.* ***C,*** *Average of fit parameter S (Asymptotic Survival Rate) for CDKL5$^{+/y}$ and CDKL5$^{-/y}$ mice. Mutants have significantly lower survival. Average values of fit parameter τ (time constant of the fit) for CDKL5$^{+/y}$ and CDKL5$^{-/y}$. CDKL5$^{-/y}$ mice have longer average time constant.* ***D,*** *Fraction of NP spines is reduced in CDKL5$^{-/y}$ mice.* ***E-F****, Images of dendritic branch (E) and quantification (F) show that CDKL5$^{-/y}$ mice have longer spines and with a thinner head.*

Figure 3. *Long term potentiation deficit in adult CDKL5$^{-/y}$ mice. Field potential amplitude normalized to pre-theta burst level is reported for CDKL5$^{-/y}$ and CDKL5$^{+/y}$ littermates. Examples of field potential waveforms before (light grey) and after (black) LTP induction are reported at the top.*

Figure 4. *Impaired synaptic function in CDKL5$^{-/y}$ mice.* ***A****, Average mEPSCs amplitude in pyramidal cells of layer V of CDKL5$^{-/y}$ and CDKL5$^{+/y}$ littermates.* ***B****, mEPSC frequency is reduced in CDKL5$^{-/y}$ mice.* ***C****, Sample traces at low (left) and high (right) magnification.* ***D****, Cumulative distribution of mEPSCs amplitude shows a small but significant reduction.* ***E****, CDKL5$^{-/y}$ mice have longer inter-event intervals.*

***Figure 5**. Reduced spine and PSD-95 positive puncta density in P27-P28 CDKL5$^{-/y}$ mice. **A**, Dendritic branch of CDKL5$^{+/y}$ and CDKL5$^{-/y}$ mice at P27, showing a decreased number of spines but not filopodia (arrows). **B**, Spine, but not filopodia density is decreased in P27 CDKL5$^{-/y}$ mice. **C**, Examples of PSD-95 staining in layer V. **D**, Punctuate synaptic PSD-95 is reduced both in superficial and deep layers.*

***Figure 6.** Selective impairment in spine elimination in P27-P28 CDKL5$^{-/y}$ mice. **A,** Images of dendritic branches of a CDKL5$^{+/y}$ and CDKL5$^{-/y}$ mice at P27 and P28. Yellow arrows indicate persistent spines, blue arrows spines that appear at P28, red arrows spines that are lost at P28. **B,** Experimental time line for in vivo imaging of young mice. **C,** Spine gain and loss between P27 and P28 in CDKL5$^{-/y}$ and CDKL5$^{+/y}$ littermates. CDKL5$^{-/y}$ mice displayed a higher fraction of lost spines than controls but normal spine gain.*

***Figure 7**. IGF-1 improves molecular deficits of CDKL5$^{-/y}$ mice. **A**, Examples of western blots for phosphorylated Ser240-244 and total S6. **B**, IGF-1 promotes Ser240-244 S6 phosphorylation. **C**, Examples of western blots of PSD-95. **D**, IGF-1 enhances PSD-95 expression.* **E** and **F**, *IGF-1 protein levels are not different in CDKL5$^{-/y}$ and CDKL5$^{+/y}$ mice. Quantification of IGF-1 levels in somatosensory cortex of P27 (**E**) and P90 mice (**F**) was performed by ELISA.*

***Figure 8**. IGF-1 treatment improves spine density and elimination in P27-P28 CDKL5$^{-/y}$ mice . **A**, Scheme of IGF-1 treatment and repeated imaging timeline. **B**, Spine and filopodia density in P27 CDKL5$^{-/y}$ or wild type littermates treated with IGF-1 or vehicle. IGF-1 rescued the spine density reduction present in vehicle treated mutants. **C**, Images of dendritic branches of CDKL5$^{-/y}$ mice at P27 and P28, top: vehicle treatment, bottom: IGF-1 treatment. Yellow arrows indicate persistent spines, blue arrows spines that appear at P28, red arrows spines that are lost at P28 (scale bar 1 μm). **D**, Spine gain and loss between P27 and P28 in CDKL5$^{-/y}$ and wild type littermates treated with IGF-1 or vehicle. Graphs show that the abnormally high loss of spines present in CDKL5$^{-/y}$ mice is rescued by IGF-1.*

***Figure 9**. IGF-1 treatment improves spine density and turnover in adult P120 CDKL5$^{-/y}$ mice. **A,** Experimental time line for in vivo imaging of adult mice. **B**, Spine density normalized to pre-treatment density (P120) is reported for CDKL5$^{-/y}$ mice treated with vehicle or IGF-1 between the first two imaging sessions (P120-P124). IGF-1 induced an increase in spine density followed by a*

decrease after treatment interruption. At all time points, IGF-1 treated mice had more spines than vehicle treated mice. ***C****, Fraction of the total number of spines gained and lost between P120 and P124 in CDKL5$^{-/y}$ treated with IGF-1 or vehicle. IGF-1 enhanced spine gain and reduced spine loss.*

Table 1. Resting potential and input resistance are unaffected by CDKL5 deletion.

Resting potential (Vm) and input resistance (R_{in}) were not statistically different in CDKL5$^{-/y}$ (n= 12 cells for CDKL5$^{+/y}$ mice, n=11 cells for CDKL5$^{-/y}$ mice; Vm t-test t(21)=-0.48 p=0.64; R_{in} t-test t(21)=-0.72 p=0.48).

	Vm (mV)	R_{in} (MΩ)
CDKL5$^{+/y}$	-60.2±1.7	152.1±36.4
CDKL5$^{-/y}$	-61.2±1.1	118.31±29.1

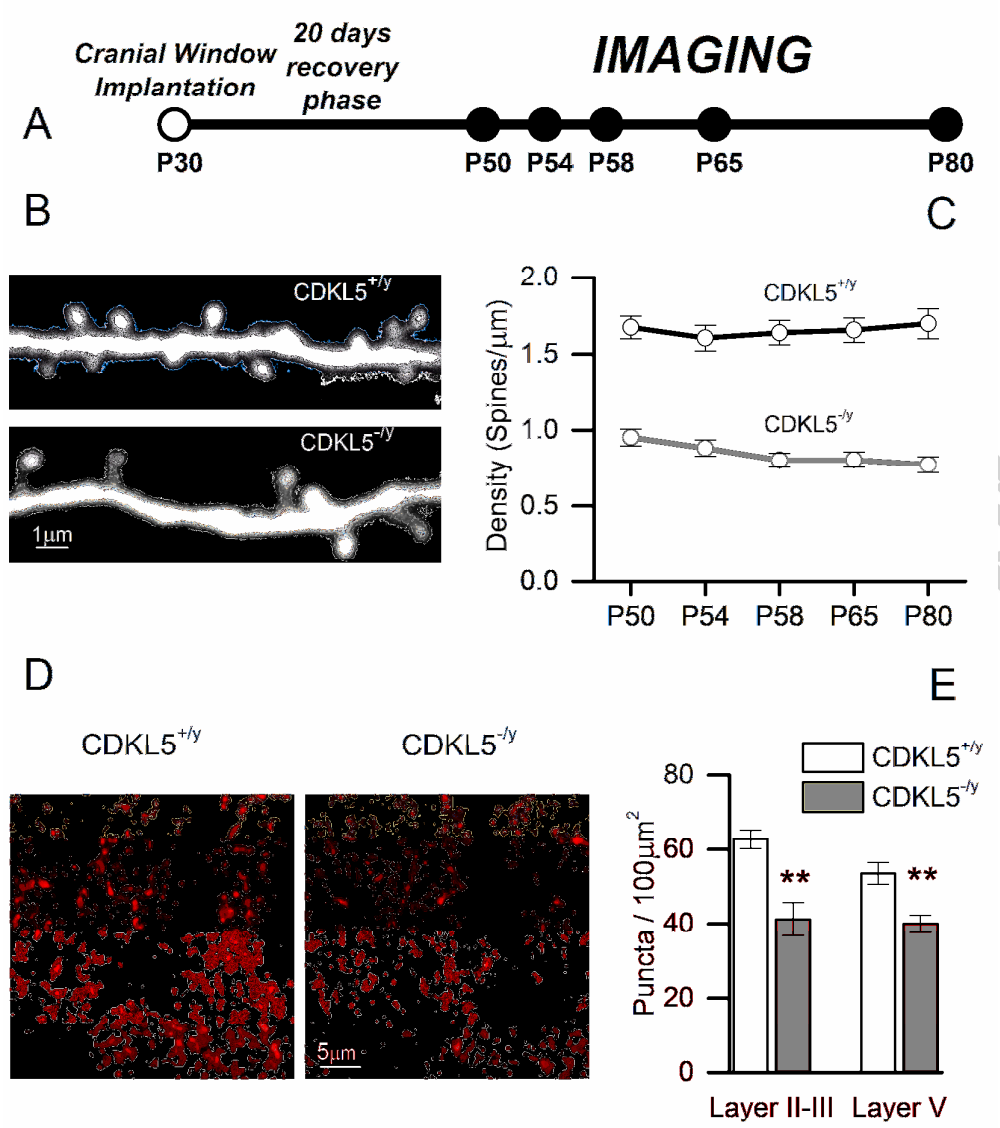
A
Cranial Window Implantation
20 days recovery phase
IMAGING
P30
P50
P54
P58
P65
P80
B
C
CDKL5+/y
CDKL5-/y
1µm
Density (Spines/µm)
2.0
1.5
1.0
0.5
0.0
P50
P54
P58
P65
P80
D
E
CDKL5+/y
CDKL5-/y
5µm
Puncta / 100µm2
80
60
40
20
0
**
**
Layer II-III
Layer V

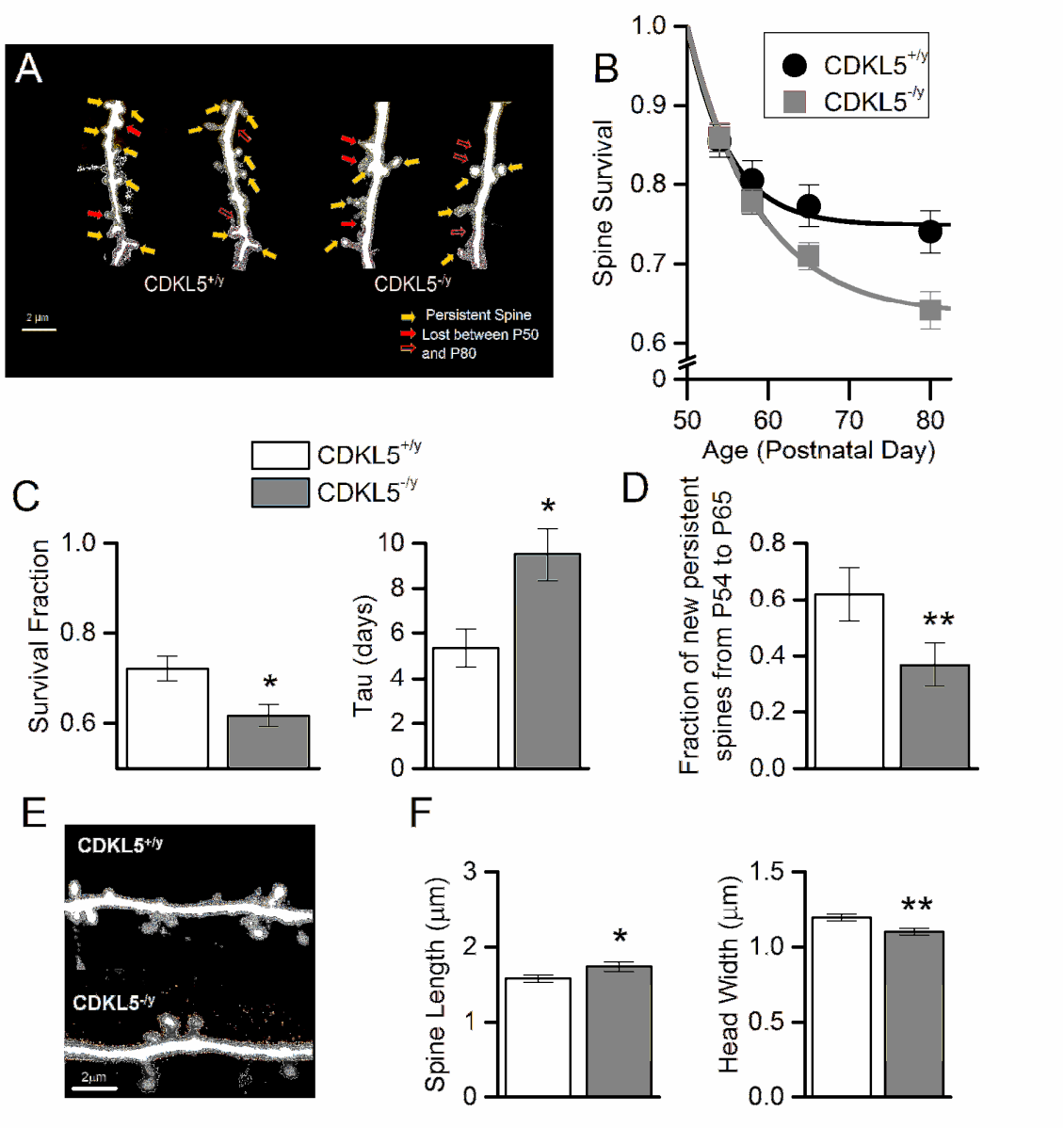
A
CDKL5+/y
CDKL5-/y
2 µm
Persistent Spine
Lost between P50 and P80
B
CDKL5+/y
CDKL5-/y
Spine Survival
1.0
0.9
0.8
0.7
0.6
0
50
60
70
80
Age (Postnatal Day)
C
CDKL5+/y
CDKL5-/y
Survival Fraction
1.0
0.8
0.6
*
Tau (days)
10
8
6
4
2
0
*
D
Fraction of new persistent spines from P54 to P65
0.8
0.6
0.4
0.2
0.0
**
E
CDKL5+/y
CDKL5-/y
2µm
F
Spine Length (µm)
3
2
1
0
*
Head Width (µm)
1.5
1.0
0.5
0.0
**

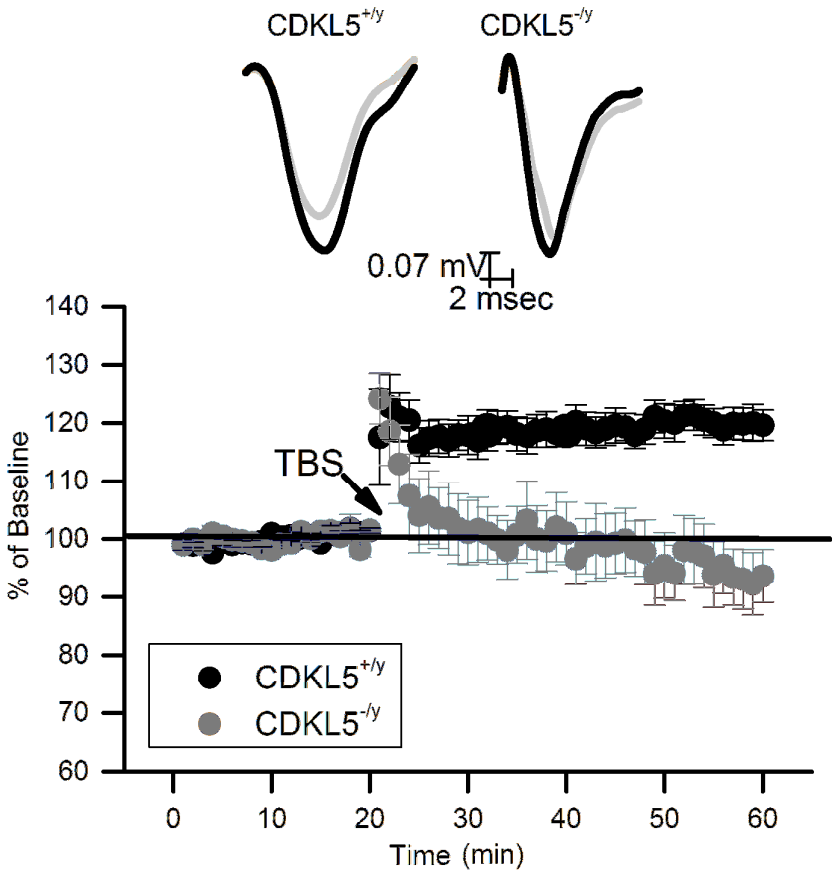

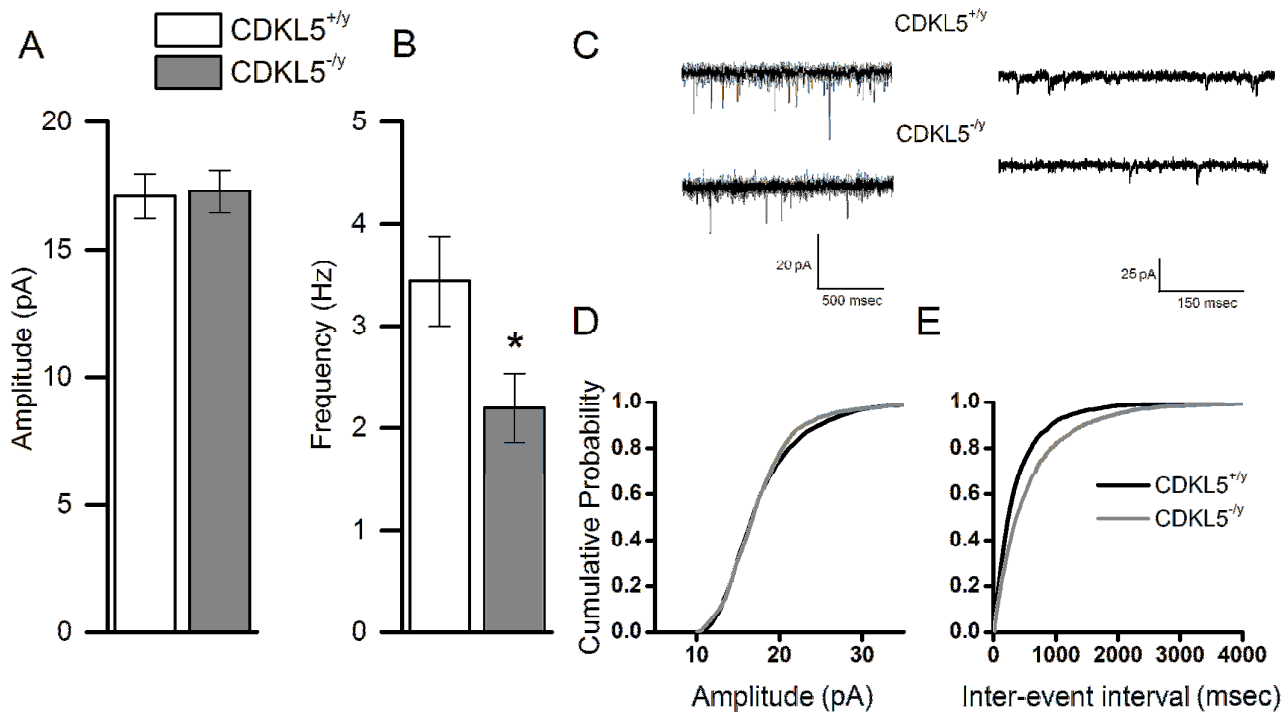

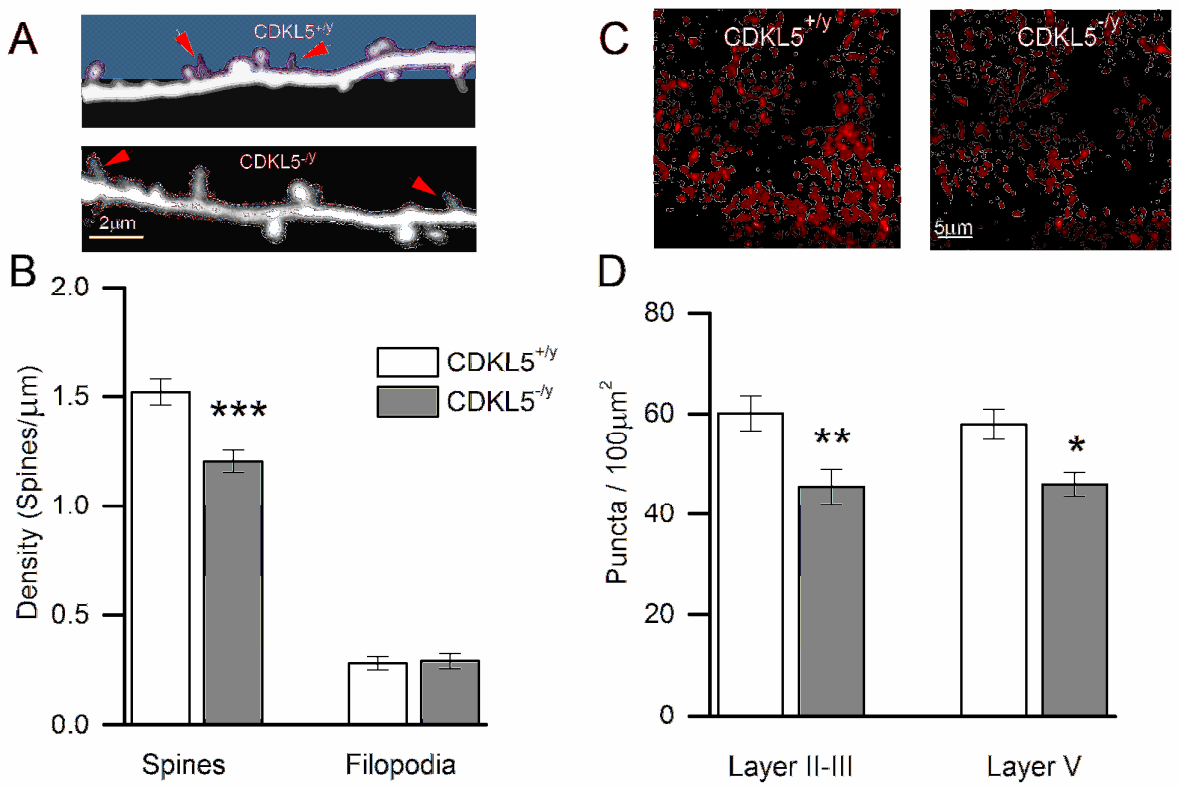
A
CDKL5+/y
CDKL5-/y
2µm
B
Density (Spines/µm)
2.0
1.5
1.0
0.5
0.0
***
CDKL5+/y
CDKL5-/y
Spines
Filopodia
C
CDKL5+/y
CDKL5-/y
5µm
D
Puncta / 100µm2
80
60
40
20
0
**
*
Layer II-III
Layer V

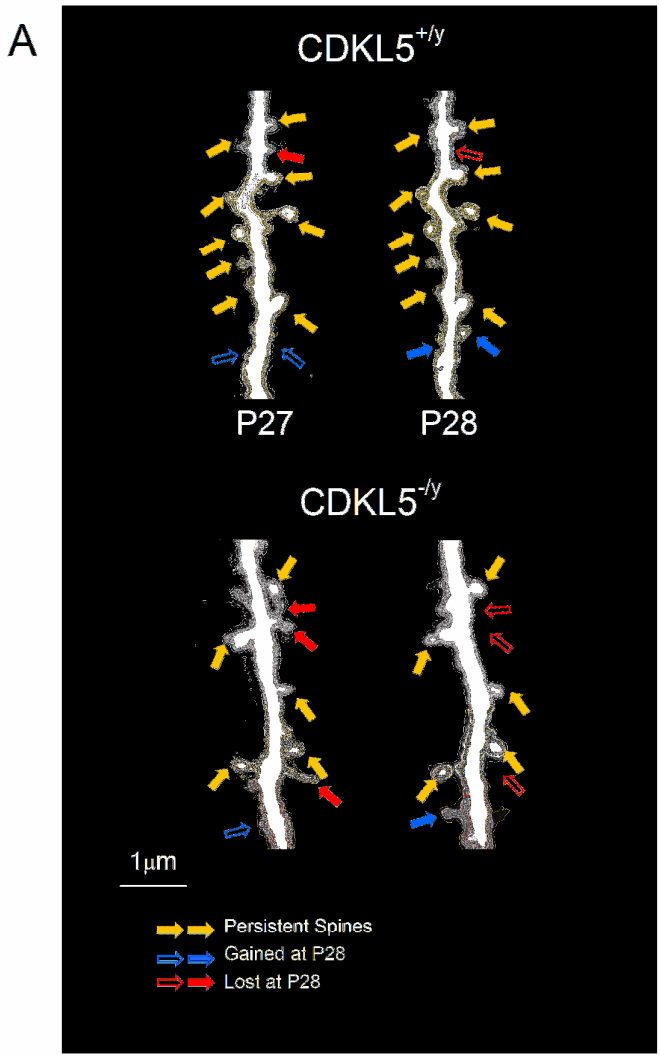
A
CDKL5+/y
P27
P28
CDKL5-/y
1µm
Persistent Spines
Gained at P28
Lost at P28

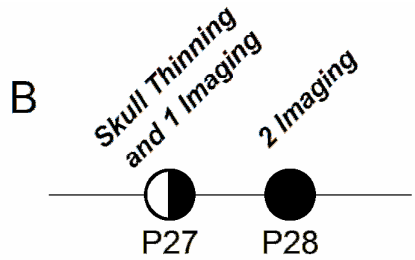
B
Skull Thinning and 1 Imaging
2 Imaging
P27
P28

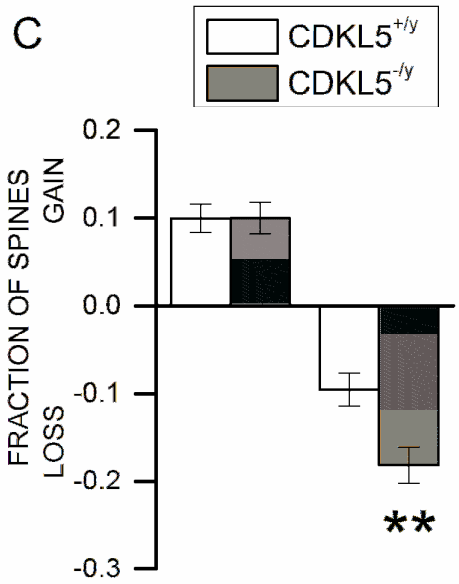
C
CDKL5+/y
CDKL5-/y
FRACTION OF SPINES
GAIN
LOSS
0.2
0.1
0.0
-0.1
-0.2
-0.3
**

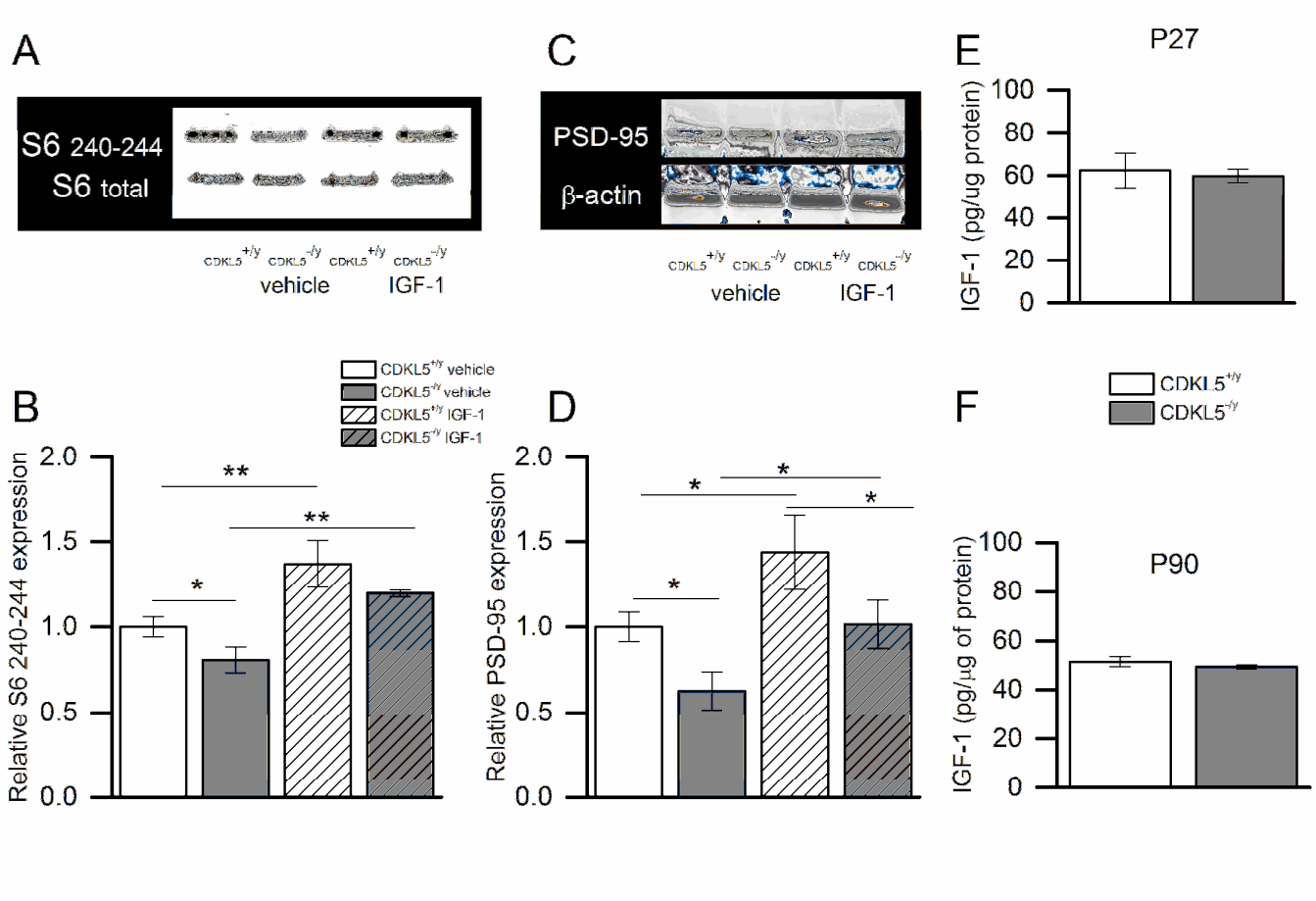
A
S6 240-244
S6 total
CDKL5+/y CDKL5-/y CDKL5+/y CDKL5-/y
vehicle
IGF-1
C
PSD-95
β-actin
CDKL5+/y CDKL5-/y CDKL5+/y CDKL5-/y
vehicle
IGF-1
E
P27
IGF-1 (pg/ug protein)
100
80
60
40
20
0
B
CDKL5+/y vehicle
CDKL5-/y vehicle
CDKL5+/y IGF-1
CDKL5-/y IGF-1
Relative S6 240-244 expression
2.0
1.5
1.0
0.5
0.0
**
**
*
D
Relative PSD-95 expression
2.0
1.5
1.0
0.5
0.0
*
*
*
*
F
CDKL5+/y
CDKL5-/y
P90
IGF-1 (pg/µg of protein)
100
80
60
40
20
0

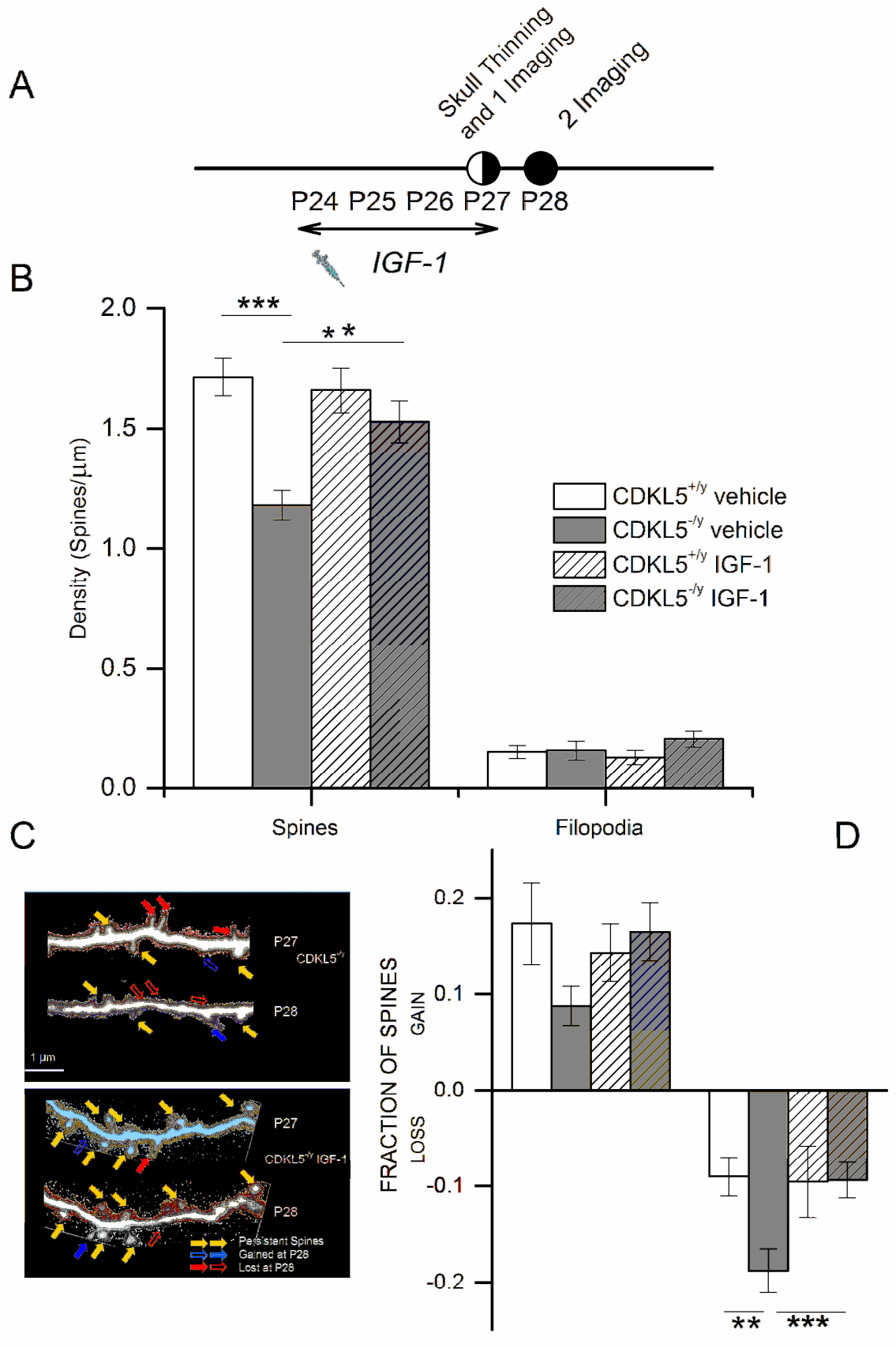
A
Skull Thinning and 1 Imaging
2 Imaging
P24 P25 P26 P27 P28
IGF-1
B
Density (Spines/µm)
2.0
1.5
1.0
0.5
0.0
***
**
CDKL5+/y vehicle
CDKL5-/y vehicle
CDKL5+/y IGF-1
CDKL5-/y IGF-1
Spines
Filopodia
C
P27
CDKL5-/y
P28
1 µm
P27
CDKL5-/y IGF-1
P28
Persistant Spines
Gained at P28
Lost at P28
D
FRACTION OF SPINES
GAIN
LOSS
0.2
0.1
0.0
-0.1
-0.2
**
***